Regular Article
pISSN: 2288-9744, eISSN: 2288-9752
Journal of Forest and Environmental Science
Vol. 38, No. 4, pp. 239-248, December, 2022
https://doi.org/10.7747/JFES.2022.38.4.239

JFES
Journal of Forest and Environmental Science

Development of Easy-to-Use Crane-Tip Controller for Forestry Crane

Ki-Duck Kim[1] and Beom-Soo Shin[1,2,*]
[1]*Department of Biosystems Engineering, Kangwon National University, Chuncheon 24341, Republic of Korea*
[2]*Interdiciplinary Program in Smart Agriculture, Kangwon National University Graduate School, Chuncheon 24341, Republic of Korea*

Abstract

Forestry crane work in a forest harvester or forwarder is regarded as one of most hard work requiring a very high level of operation skill. The operator must handle two or more multi-axes joysticks simultaneously to control the multiple manipulators for maneuvering the crane-tip to its intended location. This study has been carried out to develop a crane-tip controller which can intuitively maneuver the crane-tip, resulting in improving the productivity by decreasing the technical difficulty of control as well as reducing the workload. The crane-tip controller consists of a single 2-axis joystick and a control algorithm run on microcontroller. Lab-scale forestry crane was constructed using electric cylinders. The crane-tip control algorithm has the crane-tip follow the waypoints generated on the given path considering the dead band region using LBO (Lateral Boundary Offset). A speed control gain to change the speed of relevant cylinders relatively is applied as well. By the P (Proportional) control within the control interval of 20 msec, the average error of crane-tip control on the predefined straight path turned out to be 14.5 mm in all directions. When the joystick is used the waypoints are generated in real time by the direction signal from the joystick. In this case, the average error of path control was 12.4 mm for straight up, straight forward and straight down movements successively at a certain constant speed setting. In the slant movement of crane-tip by controlling two axes of joystick simultaneously, the movement of crane-tip was controlled in the average error of 15.9 mm when the crane-tip is moved up and down while moving toward forward direction. It concluded that the crane-tip control was possible using the control algorithm developed in this study.

Key Words: crane-tip control, forestry crane, joystick controller, path tracking, waypoints

Introduction

As a typical timber harvest system, CTL (Cut-to-length) harvest system is used worldwide. In Korea it is partially mechanized to the extent that felling and bucking operations are carried out with chain saw in the forest and shovel logging operation is done by a woodgrab attached to the excavator (Choi et al. 2018). While developed countries in forest industry such as Northern Europe achieved full mechanization in CTL harvest system by using forest harvester and forwarder which mount a corresponding working tool to the crane-tip (Morales et al. 2014; Häggström and Lindroos 2016; Nordfjell et al. 2019; López Rojas et al. 2022).

Crane work is the most time-consuming element of harvesting and forwarding as the operator must place the crane-tip mounted implements such as harvester head and pick-up equipment to the target as close as possible (Manner et al. 2017). In general, harvesting time for a single tree in the harvester is less than 1 minute, during which

Received: October 19, 2022. Revised: November 20, 2022. Accepted: November 20, 2022.

Corresponding author: Beom-Soo Shin
Department of Biosystems Engineering, Kangwon National University, Chuncheon 24341, Republic of Korea
Tel: +82-33-250-6493, Fax: +82-33-259-6651, E-mail: bshin@kangwon.ac.kr

an average of 24 functions are used and 12 decisions are made (Burman and Löfgren 2007). The physical and mental stress is considerable by repeatedly performing high-intensity precision work (Löfgren and Wikander 2009). Similarly, the forwarder operator performs a series of consecutive works repeatedly. 50% of the total forwarding work is done by the crane, and it takes about 30 seconds on average to load and unload a single piece of timber to and from the cargo box thus processing about 400 trees a day (Löfgren and Wikander 2009; Westerberg 2014).

Forestry crane work is regarded as one of most intensive work requiring a very high level of operation skill. The operator must handle two or more multi-axis joysticks simultaneously to control the position of multiple manipulators for maneuvering the crane-tip to its intended location. When the slewing axis is fixed, the crane-tip controller makes it possible for the operator to use a single 2-axes joystick which can intuitively maneuver the crane-tip on a vertical plane. This improves the productivity by lowering the technical difficulty of control as well as reducing the workload (Kim and Shin 2022). In advanced forestry countries such as Northern Europe and North America, research on path planning and path tracking of crane-tip for improved workability and robotization of timber harvesting are being actively conducted (Morales et al. 2014; Fodor et al. 2015; Kalmari 2015; La Hera et al. 2021; Jelavic et al. 2021).

Knuckle boom cranes widely used as forestry crane have RRRP (Revolute-Revolute-Revolute-Prismatic) type manipulators, where the telescopic cylinder extends the work range of horizontal and vertical movement. In this study we did not include the slewing axis (first R in RRRP type manipulator). On a vertical plane the crane-tip control is done by the boom and the arm within possible work range. Beyond the range the telescopic arm starts to be involved in the crane-tip control.

Through the preceding research (Kim and Shin 2022) we found out that the horizontal and vertical path control algorithm for the RR (Revolute-Revolute) type manipulator using only the boom and the arm was successful in an error range of 10 mm in the predefined path by using only P control as long as control interval time is less than 20 msec. Morales et al. (2014) applied PID (Proportional-Integral-Derivative) control to a RRRP type lab-scale crane (including slewing) using hydraulic cylinders. The crane-tip path control was achieved within an average error of about 28 mm. Chakraborty and Meena (2016) conducted a performance test of crane-tip control through automation of a hydraulic crane by picking up a virtual load and dropping it to a target point by a series of movement such as vertical rising, horizontal moving, and vertical lowering. There was a tracking error within 50 mm for the vertical descending path of 800 mm in distance. For this series of motions, it took 3 min for manual control and 2.2 min for automatic control to save approximately 27% of the total time.

In this study, the crane-tip control algorithm based on P control including speed control of electric cylinders was evaluated in the lab-scale RRP type crane. By developing a real time path generation method using the joystick, the feasibility of applying the crane-tip controller to forestry crane would be evaluated through various path tacking tests in horizontal, vertical, and slant paths.

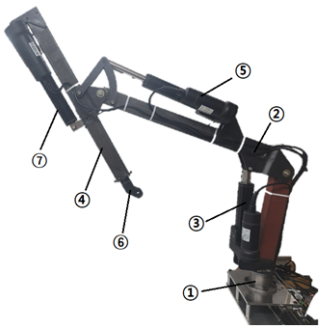

Fig. 1. Lab-scale crane used in the study (① Slewing plate, ② Boom, ③ Boom cylinder, ④ Arm, ⑤ Arm cylinder, ⑥ Telescopic arm, ⑦ Telescopic arm cylinder).

Table 1. Specifications of electrical cylinders used in cranes

Items		Specification
Spindle type		ACME screw
Operating voltage (V)		24VDC
Typical speed (mm/s)	No load	29.5
	With load	27
Stroke (mm)	Slewing	100
	Boom	140
	Arm	190
	Telescopic arm	225

Materials and Methods

Experimental forestry crane

Dimension of crane

A lab-scale crane was constructed in 1/3 scale of an actual forestry crane as shown in Fig. 1. It is RRRP type where four electric cylinders drive each manipulator for slewing, arm, boom and telescopic arm. These electric cylinders are driven by 24V DC motor where the speed of motor is controlled by its duty ratio, and its specifications are presented in Table 1.

Kinematic analysis of Forestry crane

D-H (Denavit Hartenberg) parameter

To define the kinematic characteristics of the crane shown in Fig. 2, the D-H parameters of the crane used are presented in Table 2 (Chakraborty and Meena 2016). O_0 is a joint for slewing as a revolute joint. O_1 and O_2 are revolute joints for boom and arm, respectively. O_3 is a prismatic joint as a constant that occurs when connecting the boom and arm without mechanical interference. O_4 is a prismatic joint that expresses the distance to the end effector including the telescopic cylinder stroke.

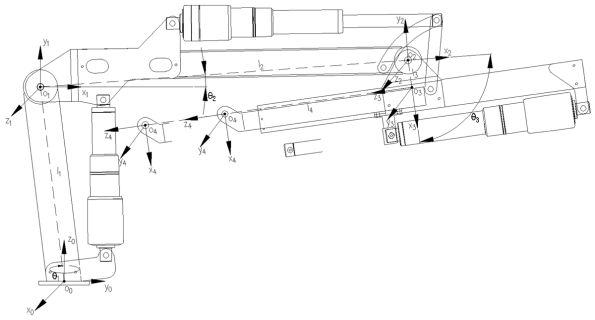

Fig. 2. Coordinates of crane manipulator for kinematics.

Forward kinematics

To figure out the position of the end effector, forward kinematics was used on the coordinate system defined as shown in Fig. 2. The position of the crane-tip, which is the end effector, based on the coordinate system of the slewing joint (O_0) is the product of the transformation matrix for each joint as in the eq. (1), and can be expressed as T_0^4 (Jung 2019).

$$T_0^4 = A_0^1 A_1^2 A_2^3 A_3^4 \tag{1}$$

where,

$$A_0^1 = \begin{bmatrix} cos\theta_1 & -cos\alpha_1 sin\theta_1 & sin\alpha_1 sin\theta_1 & a_1 cos\theta_1 \\ sin\theta_1 & cos\alpha_1 cos\theta_1 & -sin\alpha_1 cos\theta_1 & a_1 sin\theta_1 \\ 0 & sin\alpha_1 & cos\alpha_1 & d_1 \\ 0 & 0 & 0 & 1 \end{bmatrix} = \begin{bmatrix} cos\theta_1 & 0 & sin\theta_1 & -51.8427 cos\theta_1 \\ sin\theta_1 & 0 & -cos\theta_1 & -51.8427 sin\theta_1 \\ 0 & 1 & 0 & 422.2247 \\ 0 & 0 & 0 & 1 \end{bmatrix}$$

$$A_1^2 = \begin{bmatrix} cos\theta_2 & -cos\alpha_2 sin\theta_2 & sin\alpha_2 sin\theta_2 & a_2 cos\theta_2 \\ sin\theta_2 & cos\alpha_2 cos\theta_2 & -sin\alpha_2 cos\theta_2 & a_2 sin\theta_2 \\ 0 & sin\alpha_2 & cos\alpha_2 & d_2 \\ 0 & 0 & 0 & 1 \end{bmatrix} = \begin{bmatrix} cos\theta_2 & -sin\theta_2 & 0 & 803.6246 cos\theta_2 \\ sin\theta_2 & cos\theta_2 & 0 & 803.6246 sin\theta_2 \\ 0 & 0 & 1 & 0 \\ 0 & 0 & 0 & 1 \end{bmatrix}$$

$$A_2^3 = \begin{bmatrix} cos\theta_3 & -cos\alpha_3 sin\theta_3 & sin\alpha_3 sin\theta_3 & a_3 cos\theta_3 \\ sin\theta_3 & cos\alpha_3 cos\theta_3 & -sin\alpha_3 cos\theta_3 & a_3 sin\theta_3 \\ 0 & sin\alpha_3 & cos\alpha_3 & d_3 \\ 0 & 0 & 0 & 1 \end{bmatrix} = \begin{bmatrix} cos\theta_3 & 0 & sin\theta_3 & 59.5 cos\theta_3 \\ sin\theta_3 & 0 & -cos\theta_3 & 59.5 sin\theta_3 \\ 0 & 1 & 0 & 0 \\ 0 & 0 & 0 & 1 \end{bmatrix}$$

$$A_3^4 = \begin{bmatrix} cos\theta_4 & -cos\alpha_4 sin\theta_4 & sin\alpha_4 sin\theta_4 & a_4 cos\theta_4 \\ sin\theta_4 & cos\alpha_4 cos\theta_4 & -sin\alpha_4 cos\theta_4 & a_4 sin\theta_4 \\ 0 & sin\alpha_4 & cos\alpha_4 & d_4 \\ 0 & 0 & 0 & 1 \end{bmatrix} = \begin{bmatrix} 1 & 0 & 0 & 0 \\ 0 & 1 & 0 & 0 \\ 0 & 0 & 1 & 412 + l \\ 0 & 0 & 0 & 1 \end{bmatrix}$$

Table 2. D-H parameters of manipulators

Joint i	θ_i	α_i	d_i	a_i
0 (R)	0	0	0	0
1 (R)	θ_1	90	422.2247	-51.8427
2 (R)	θ_2	0	0	803.6246
3 (P*)	θ_3	90	0	59.5
4 (P)	0	0	$412 + l$	0

where, θ_i : the angle between x_{i-1} and x_i measured about z_i, variable.
α_i : the angle between z_i and z_{i+1} measured about x_i, constant.
d_i: the distance from x_{i-1} and x_i measured along z_i, constant.
a_i: the distance from z_i and z_{i+1} measured along x_i, constant.
l: the stroke of telescopic arm cylinder, variable.
*Fixed prismatic joint due to linkage.

By substituting the D-H parameter variable into the eq. (1), it is expressed as the entire transformation matrix as in eq. (2). P_x, P_y, P_z are coordinates in space indicating the position of the end effector.

$$T_0^4 = \begin{bmatrix} r_{11} & r_{12} & r_{13} & P_x \\ r_{21} & r_{22} & r_{23} & P_y \\ r_{31} & r_{32} & r_{33} & P_z \\ 0 & 0 & 0 & 1 \end{bmatrix} \quad (2)$$

where,

$r_{11} = cos\theta_1 \cos(\theta_2+\theta_3)$

$r_{12} = sin\theta_1$

$r_{13} = cos\theta_1 \sin(\theta_2+\theta_3)$

$r_{21} = sin\theta_1 \cos(\theta_2+\theta_3)$

$r_{22} = -cos\theta_1$

$r_{23} = sin\theta_1 \sin(\theta_2+\theta_3)$

$r_{31} = \sin(\theta_2+\theta_3)$

$r_{32} = 0$

$r_{33} = -cos(\theta_2+\theta_3)$

$P_x = -51.8427 cos\theta_1 + 803.6246 cos\theta_1 cos\theta_2 + 59.5 \cos\theta_1 cos(\theta_2+\theta_3) + (412+l) cos\theta_1 \sin(\theta_2+\theta_3)$

$P_y = -51.8427 sin\theta_1 + 803.6246 sin\theta_1 cos\theta_2 + 59.5 \sin\theta_1 \cos(\theta_2+\theta_3) + (412+l) sin\theta_1 \sin(\theta_2+\theta_3)$

$P_z = 422.2247 + 803.6246 sin\theta_2 + 59.5 \sin(\theta_2+\theta_3) - (412+l) \cos(\theta_2+\theta_3)$

Inverse kinematics

Inverse kinematic analysis was analytically performed to calculate the angle data of each joint. θ_1, θ_2, θ_3 can be obtained through the following eq. (3), (4) and (5) (Craig 1989).

$$\theta_1 = \text{atan}\left(\frac{P_y}{P_x}\right) - \text{atan}\left(\frac{d_2+d_3}{\pm\sqrt{P_x^2+P_y^2+(d_2+d_3)^2}}\right) \quad (3)$$

$$\theta_2 = \text{atan}\left(\frac{sin\theta_2}{cos\theta_2}\right) \quad (4)$$

$$\theta_3 = \text{atan}\left(\frac{K}{\pm\sqrt{(a_3+a_4)^2+d_4^2-K^2}}\right) - \text{atan}\left(\frac{a_3+a_4}{d_4}\right) \quad (5)$$

where,

$$K = \frac{P_x^2+P_y^2+P_z^2+a_1^2+d_1^2-2P_x a_1 cos\theta_1 - 2P_y a_1 sin\theta_1 - 2P_z d_1 - a_2^2 - a_3^2 - a_4^2 - d_2^2 - d_3^2 - d_4^2 - 2a_3a_4 - 2d_2d_3}{2a_2}$$

$$cos\theta_2 = \frac{(a_2+a_3cos\theta_3+a_4cos\theta_3+d_4sin\theta_3)(P_x cos\theta_1 + P_y sin\theta_1 - a_1) + (P_z-d_1)(a_3 sin\theta_3 + a_4 sin\theta_3 - d_4 cos\theta_3)}{((P_x cos\theta_1 + P_y sin\theta_1 - a_1)^2 + (P_z-d_1)^2)}$$

$$sin\theta_2 = \frac{-(a_3 sin\theta_3 + a_4 sin\theta_3 - d_4 cos\theta_3)(P_x cos\theta_1 + P_y sin\theta_1 - a_1) + (P_z-d_1)(a_2+a_3 cos\theta_3 + a_4 cos\theta_3 + d_4 sin\theta_3)}{((P_x cos\theta_1 + P_y sin\theta_1 - a_1)^2 + (P_z-d_1)^2)}$$

When the value of each joint is calculated for a target position by the result of the kinematic analysis, the values of θ_2 and θ_3 are changed according to the length of the telescopic arm. In case of short-distance movement, the short stroke of the telescopic arm is more desirable. If the position of crane-tip is not covered by the current stroke of the telescopic arm, the range must be extended by increasing the stroke of the telescopic arm (Prorok 2003). When the telescopic arm needs to be involved, θ_2 and θ_3 are recalculated within the controllable range by increasing the stroke of the telescopic arm by 5 mm.

Workable space analysis

The slewing axis of the crane is independently controlled in operation area (Kim and Shin 2022). In this study, the slewing axis was fixed while the stroke of the telescopic arm cylinder changed by 25% intervals shown in Fig. 3, and joint angles of arm and boom increased by 3 degrees, the positions of the crane-tip on a vertical plane were expressed in terms of P_y, P_z(The Math Works, Inc. R2019b).

The largest rectangular area was set for the vertical and horizontal movable range to be used in the experiment within the operation area of the entire crane-tip according to

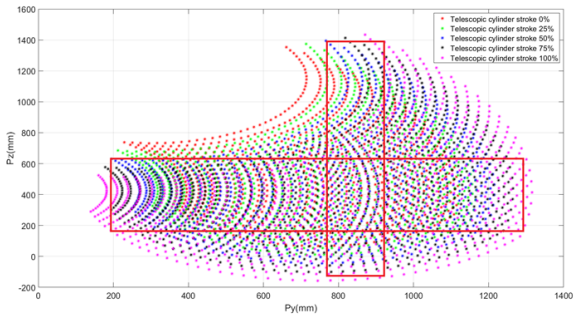

Fig. 3. Operation area of crane-tip according to telescopic cylinder stroke.

the Korean Standard (KS B ISO 9283:1998). Two points (400, 600) and (1,200, 600) for horizontal movement and two points (900, 200) and (900, 1200) for vertical movement were selected as start and stop positions, respectively, in the section where the telescopic arm cylinder is involved in the crane-tip control. These two selected points were used for performance evaluation.

Control system

For the control of the crane-tip using a joystick, a single 2-axes joystick equipped with CAN (Controller Area Network) communication was added to the existing control system (Kim and Shin 2022). The joystick outputs proportional signals for both forward/backward and upward/downward directions. The overall control system of the crane with the added joystick is shown in Fig. 4. The position data from the linear displacement sensor attached to each cylinder and the joystick signal are transmitted to the main ECU (Electronic Control Unit) through the CAN bus. A command to operate each cylinder is transmitted to the DC motor driver based on the crane-tip control algorithm in the main ECU. In the existing crane-tip control algorithm, it was possible to generate waypoints on the path in advance based on two fixed points. In the case of using a joystick, it is not possible to create waypoints in advance. Therefore, in this study, we developed an algorithm to generate a waypoint in real time in the direction to move according to the direction signal of the joystick (Fig. 5).

Performance evaluation

Crane-tip control on predefined horizontal/vertical path

In the case of following a path from the current position to an arbitrary target point, the strokes of the boom cylinder, arm cylinder, and telescopic arm cylinder at each waypoint are changed each time. Within a certain range that the telescopic arm cylinder is not engaged in the crane-tip control, the displacement of the arm cylinder is greater than the displacement of the boom cylinder on the horizontal movement while the displacement of the boom cylinder is greater than the displacement of the arm cylinder on the vertical movement. However, in the range where the telescopic arm cylinder affects the crane-tip control, the displacement of the telescopic arm cylinder is significantly greater than the displacement of the boom cylinder and the arm cylinder.

When either boom or arm cylinder reaches its target position first, an overshoot or undershoot could occur on the path. The crane-tip control algorithm in the preceding study (Kim and Shin 2022) was applied to slowly control the cylinder with relatively small displacement, and the telescopic arm cylinder was set so that it could always be controlled at the maximum speed.

The experiment was repeated 3 times for horizontal movement (forward/backward) and vertical movement (up/down) under the condition of LBO radius of 5 mm, respectively. The result of performance evaluation was de-

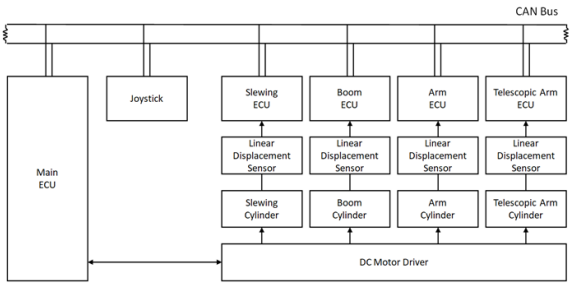

Fig. 4. Diagram of electronic control system in crane.

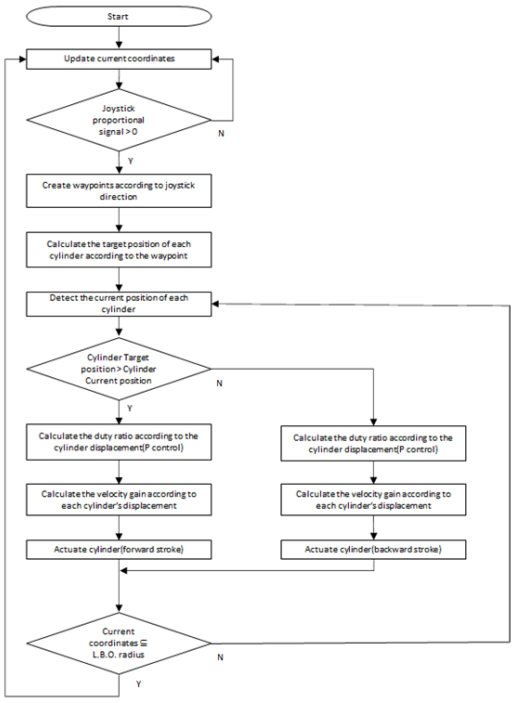

Fig. 5. Crane-tip control algorithm using joystick.

fined in terms of positioning accuracy expressed as an average error and the time required to perform control by referring to the posture accuracy of the Korean Standard (KS B ISO 9283:1998).

Crane-tip control with a joystick

To change the speed of each cylinder at the same rate according to the degree of proportional signal of the joystick, a joystick proportional gain with the maximum value of 1 was additionally applied to the crane-tip control algorithm to which the speed gain was applied. After that, the average error and the time required for each direction according to the joystick proportional gain of 0.1 interval were measured three times. In addition, one-way ANOVA was performed at a significance level of 5% by using the Statistical data analysis tool add-in for Microsoft Excel (Analysis-it Software, Ltd., Standard Edition, Leeds, UK) to investigate the correlation between the time required for each direction and the average error according to the applied joystick proportional gain.

Finally, to investigate the crane-tip control algorithm where the waypoint generated in real time according to the direction signal of the joystick, performance evaluation tests according to the joystick signal simulating linear movement and slant movement at an arbitrary position were carried out 3 times, respectively.

Results and Discussion

Performance of crane-tip control algorithm

The crane-tip control algorithm with speed gain was applied to make the boom and arm cylinders reach each target position at the same time. Under the condition of LBO radius of 5 mm, the lead time and error for horizontal and vertical movements were measured as presented in Table 3.

Table 3. Lead time and error according to crane-tip control algorithm

Direction	Lead time (ms)	Error (mm)
Forward	11,147±75	14.018±0.306
Backward	11,193±81	13.915±0.216
Upward	8,507±133	14.825±0.228
Downward	8,760±196	15.206±0.144

The crane-tip moved 800 mm in the horizontal movement and 1,000 mm in the vertical movement. The lead time required in the horizontal movement was longer. It was because the stroke (125 mm) of the telescopic arm cylinder required for horizontal movement was longer than the stroke (80 mm) of the telescopic arm cylinder for vertical movement. Also, compared to horizontal movement, the average error tended to increase by about 1 mm in the vertical movement. It was judged that this was caused by an overshoot due to an increase in the moment of inertia applied to the boom joint as the placement of the boom and arm became straight at the highest position. The trajectory of the actual crane-tip movement was investigated further (Fig. 6).

The actual trajectory was observed that the crane-tip vibrated badly regardless of the moving direction. It was analyzed that this happened because the speed between the cylinders did not match as the speed of DC motor could not be

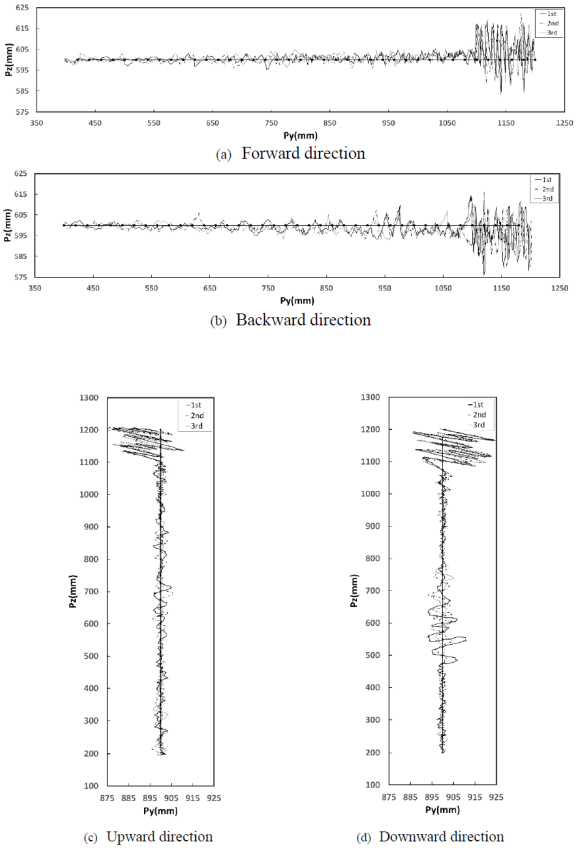

(a) Forward direction

(b) Backward direction

(c) Upward direction

(d) Downward direction

Fig. 6. Control pattern of crane-tip control algorithm.

controlled below the duty ratio of 25%. Further severer fluctuation was observed in the later part of movement. This part was a section where the telescopic arm cylinder started to be involved in the crane-tip control. The telescopic arm cylinder moved slower than the boom and arm cylinders did as well as it was controlled discretely by 5 mm. Nevertheless the crane used in the study was controlled within an error range of up to 25 mm along the horizontal path of 600 mm on the Z-axis, and up to 25 mm along the vertical path of 900 mm on the Y-axis as well.

When the same algorithm is applied to the actual forestry crane using hydraulic cylinders that do not have a limit on the minimum speed of cylinder operation, the performance is expected to be better in the average error and the time required.

Table 4. Lead time and error according to joystick proportional gain

Direction	Joystick proportional gain	Lead time (ms)	Error (mm)
Forward	0.4	12,153±57.349	14.672±0.089
	0.5	22,840±99.331	14.591±0.172
	0.6	18,853±61.824	14.391±0.111
	0.7	16,013±33.993	14.246±0.110
	0.8	13,827±94.281	14.272±0.143
	0.9	12,487±41.096	14.051±0.183
	1	11,147±75.425	14.018±0.306
Backward	0.4	28,867±92.856	14.629±0.157
	0.5	22,533±171.529	14.537±0.044
	0.6	18,600±123.288	14.338±0.131
	0.7	15,760±71.181	14.196±0.125
	0.8	13,720±43.205	14.170±0.060
	0.9	12,393± 77.172	14.063±0.128
	1	11,193±80.554	13.915±0.216
Upward	0.4	23,007±131.993	15.709±0.208
	0.5	17,667±83.799	15.563±0.233
	0.6	14,467±18.856	15.245±0.146
	0.7	12,127±80.554	15.148±0.263
	0.8	10,600±58.878	15.105±0.411
	0.9	9,447±33.993	15.044±0.310
	1	8,507±133.000	14.825±0.228
Downward	0.4	22,813±65.997	15.539±0.252
	0.5	17,607±61.824	15.527±0.040
	0.6	14,507±77.172	15.363±0.053
	0.7	12,180±32.660	15.332±0.269
	0.8	10,767±73.636	15.186±0.186
	0.9	9,587±154.344	15.166±0.308
	1	8,760±195.959	15.206±0.144

Performance of crane-tip control with a joystick

To change the speed of the boom, arm, and telescopic arm cylinders at the same rate according to the degree of proportional signal of the joystick, a joystick proportional gain with the maximum value of 1 was applied to the formula to determine cylinder speed. The error and the lead time according to the joystick proportional gain were measured as presented in Table 4.

The overall average error was 14.787 mm, and the error increased up to 6%, based on a joystick proportional gain of 1, as the joystick proportional gain decreased. The lead time increased at the same rate within the error range of about 8% as the joystick proportional gain decreased.

To check the correlation between the lead time and the error as the joystick proportional gain changes, one-way ANOVA test was done at the significance level of 5% as presented in Table 5.

The average error in the path tracking was related to the joystick proportional gain in the vertical movement, but not in the horizontal movement. The lead time turned out to be related with the joystick proportional gain for all directions. It was determined that a joystick proportional gain could be used to control the speed of the crane-tip using the joystick. However, it was necessary to further analyze the mean error on a path in which several directions were mixed.

To check the performance of algorithm that generates the waypoint in the direction of movement in real time according to the direction signal of the joystick, we generated simulated joystick signals for 10 sec up, 8 sec forward, and 13 sec down at a constant speed (50% of max. speed) to move the crane-tip starting from an arbitrary position (800, 200) as shown in Fig. 7a. The trajectory of crane-tip movement repeated three times are shown in Fig. 7b.

As a result, when upward-forward-downward commands were consecutively applied, the crane-tip moved 900 mm upward, 175 mm forward and 900 mm downward. Even though the moving distance was the same for up and down movements, the required time was different. Because the displacement that each cylinder needs to move according to the coordinates in space was different.

Excessive fluctuation was also observed in the region marked by a circle in Fig. 7b, where the telescopic arm cylinder worked. Three replicated trials showed an average error of 12.506 mm, 12.279 mm, and 12.375 mm, respectively.

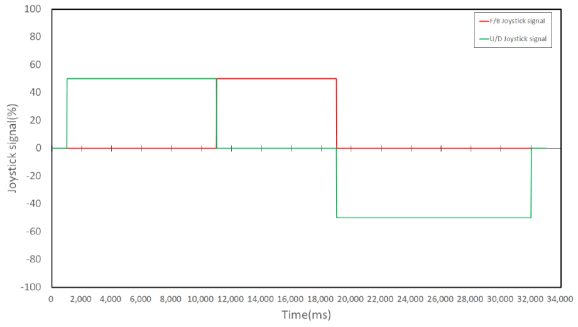

(a) Joystick control (input)

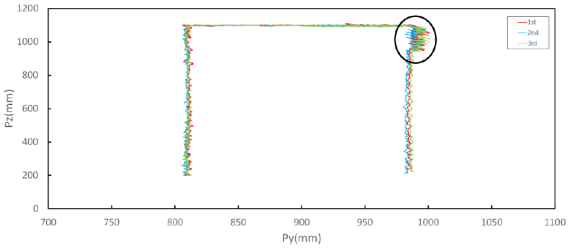

(b) Trajectory of crane-tip (output)

Fig. 7. Linear movement of crane-tip by simulated joystick signal.

Table 5. One-way ANOVA for the error and lead time by joystick proportional gain (α=0.05)

Parameter	Factor	SS	DF	MS	F	p
Forward	Error	1.124	6	0.187	4.169	0.013
	Lead time	740.628	6	12.438	16,745.465	0.000
Backward	Error	1.168	6	0.195	7.204	0.001
	Lead time	716.603	6	119.434	7,674.760	0.000
Upward	Error	1.683	6	0.281	2.596	0.066
	Lead time	480.247	6	80.041	6,968.756	0.000
Downward	Error	0.440	6	0.073	1.180	0.371
	Lead time	453.567	6	75.594	4,258.272	0.000

Table 6. The error according to joystick signal

Joystick signal (%)	Error (mm)
30	12.557±0.119
50	12.538±0.036
70	12.633±0.057

Table 7. One-way ANOVA for the error by joystick signal (α=0.05)

Parameter	Factor	SS	DF	MS	F	p
Joystick signal	Error	0.015	2	0.008	0.814	0.487

In case of controlling the crane-tip according to the joystick signal, since the control in multiple directions is performed, it would be more reliable to investigate the relationship between joystick proportional gain and the path tracking error. Therefore, additional experiments were carried out with different rates of proportional gain as presented in Table 6, and a one-way ANOVA was tested at a significance level of 5% (Table 7).

One-way ANOVA test has confirmed that there was no relationship between the joystick signal and the mean error, which meant that the crane-tip moving speed was not related with the mean error. Therefore, it has been verified that the joystick signal can be used as an input signal for controlling only the moving speed of the crane-tip.

In actual crane work, to move the crane-tip toward a certain position the operator can operate a stick in 2-axis joystick independently to move the crane-tip vertically or horizontally. Or if he operates both sticks simultaneously then the crane-tip moves obliquely. Simulated joystick signal was generated by operating the upward stick for 4 sec and the downward stick 10 sec while maintaining the forward stick at a position (Fig. 8a) and the crane-tip movement started from an arbitrary position (900, 200). The trajectory of crane-tip movement was shown in Fig. 8b.

Fig. 8b showed that the crane-tip moved along the inclined straight line. As shown in the earlier figures, some fluctuation occurred in the region where the telescopic arm cylinder was involved in the crane-tip control. Finally, it was confirmed that control in the slant movement was possible within the average error of 15.606 mm, 16.318 mm, and 15.834 mm for three repeated trials.

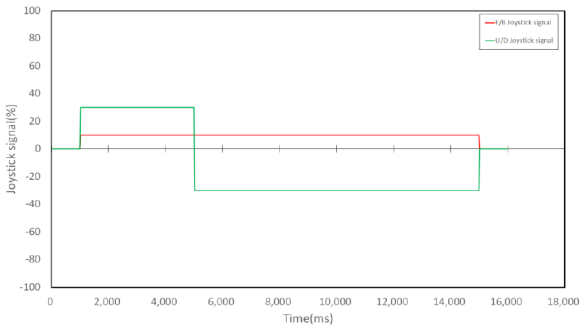

(a) Joystick signal (input)

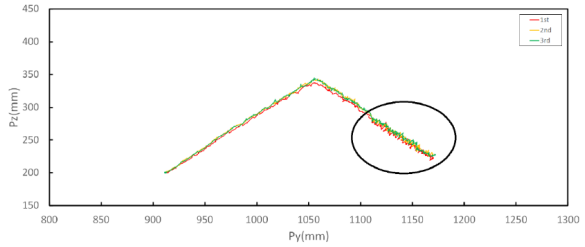

(b) Trajectory of crane-tip (output)

Fig. 8. Slant movement of crane-tip by simulated joystick signal.

Conclusion

Crane work in harvesters or forwarders, classified as high-performance forestry machines, needs high-difficulty technology that requires complex control of multi-axis joysticks. Accordingly, an easy-to-use crane-tip controller using a single 2-axis joystick was developed to improve work productivity, and a crane-tip algorithm was developed for RRP type crane. A lab-scale forestry crane driven by electric cylinders was constructed and the control performance was evaluated.

On predefined path when the target point was determined in advance the crane-tip tracks the waypoints within LBO. Like the previous research (Kim and Shin 2022) the P-control was applied in the control time of 20 msec. Speed gain was also applied to the boom and the arm cylinders while its maximum speed was maintained in the telescopic arm cylinder.

To use the joystick for the crane-tip control, a real time waypoint generation algorithm was developed according to the joystick proportional gain. When the crane-tip was moved upward, forward, and downward consecutively, the average error was 12.387 mm. In the similar way we could

control the slant movement within the average error of 15.919 mm.

In conclusion the easy-to-use crane-tip controller developed in the study was feasible in controlling RRP type manipulator within the acceptable range of path tracking error. Since the crane-tip is intuitively controlled, it is expected that the beginner operator can operate the crane system without long-term training as well as the work load is considerably reduced for skillful operator.

Acknowledgements

This study was supported by the research grant of Kangwon National University in 2022.

References

Burman L, Löfgren B. 2007. Human-Machine interaction improvements of forest machines. In: Forest Engineering Conference; Quebec, Canada; Oct 1-4, 2007.

Chakraborty S, Meena R. 2016. Saving time by tip control & automation of knuckle and boom hydraulic crane. Int J Hybrid Inf Technol 9: 235-254.

Choi YS, Cho MJ, Mun HS, Kim DH, Cha DS, Han SK, Oh JH. 2018. Analysis on Yarding Productivity and Cost of Tower-Yarder Based on Excavator Using Radio-Controlled Double Clamp Carriage. J Korean Soc For Sci 107: 266-277.

Craig JJ. 1989. Introduction to Robotics: Mechanics and Control. 2nd ed. Addison-Wesley Reading, Boston, MA.

Fodor S, Vázquez C, Freidovich L. 2015. Automation of slewing motions for forestry cranes. In: 15th International Conference on Control, Automation and Systems; Busan, Korea; Oct 13-16, 2015. pp 796-801.

Häggström C, Lindroos O. 2016. Human, technology, organization and environment - a human factors perspective on performance in forest harvesting. Int J For Eng 27: 67-78.

KS B ISO 9283:1998. 1998. Manipulating Industrial Robots-Performance Criteria and Related Test Methods. Korean Industrial Standards, pp 8-16.

Jelavic E, Jud D, Egli P, Hutter M. 2021. Towards Autonomous Robotic Precision Harvesting: Mapping, Localization, Planning and Control for a Legged Tree Harvester. arXiv doi: 10.48550/arXiv.2104.10110.

Jung S. 2019. Robotics. 5th ed. Gyomoon, Paju.

Kalmari J. 2015. Nonlinear model predictive control of a hydraulic forestry crane. PhD thesis. Aalto University, Helsinki, Finland. (in English)

Kim KD, Shin BS. 2022. A Feasibility Study in Forestry Crane-Tip Control Based on Kinematics Model (1): The RR Manipulator. J Korean Soc For Sci 111: 287-301.

La Hera P, Morales DO, Mendoza-Trejo O. 2021. A study case of Dynamic Motion Primitives as a motion planning method to automate the work of forestry cranes. Comput Electron Agric 183: 106037.

Löfgren B, Wikander J. 2009. Kinematic control of redundant knuckle booms. Int J For Eng 20: 22-30.

López Rojas AD, Mendoza-Trejo O, Padilla-García EA, Morales DO, Cruz-Villar CA, La Hera P. 2022. Design, rapid manufacturing and modeling of a reduced-scale forwarder crane with closed kinematic chain. Mech Based Des Struct Mach doi: 10.1080/15397734.2022.2063889. [Epub ahead of print]

Manner J, Gelin O, Mörk A, Englund M. 2017. Forwarder crane's boom tip control system and beginner-level operators. Silva Fenn 51: 1717.

Nordfjell T, Öhman E, Lindroos O, Ager B. 2019. The technical development of forwarders in Sweden between 1962 and 2012 and of sales between 1975 and 2017. Int J For Eng 30: 1-13.

Morales OD, Westerberg S, La Hera PX, Mettin U, Freidovich L, Shiriaev AS. 2014. Increasing the level of automation in the forestry logging process with crane trajectory planning and control. J Field Robotics 31: 343-363.

Prorok K. 2003. Crane-tip control of a hydraulic crane: a new approach. Umeå University, Umeå.

The MathWorks, Inc. 2019. MATLAB (Version 2019b). https://www.mathworks.com/.

Westerberg S. 2014. Semi-automating forestry machines: motion planning, system integration, and human-machine interaction. PhD thesis. Umeå University, Umeå, Sweden. (in English)